

Supplementary material for:

**“Mapping the horizontal and vertical distributions of pigments  
within canopies of Ginkgo plantation based on UAV-borne  
LiDAR, hyperspectral data by coupling PROSAIL model”**

by Shiyun Yin <sup>1,†</sup>, Kai Zhou <sup>1,†</sup>, Lin Cao <sup>1,\*</sup> and Xin Shen <sup>1</sup>

1 Co-Innovation Center for Sustainable Forestry in Southern China, Nanjing Forestry University, Nanjing, Jiangsu, China

210037; [yshiyun@njfu.edu.cn](mailto:yshiyun@njfu.edu.cn) (S.Y.); [kaizhou@njfu.edu.cn](mailto:kaizhou@njfu.edu.cn) (K.Z.); [xinshen@njfu.edu.cn](mailto:xinshen@njfu.edu.cn) (X.S.)

\* Correspondence: [lincao@njfu.edu.cn](mailto:lincao@njfu.edu.cn)

† These authors contributed equally to this work and shared first authorship.

**Table S1.** Summary of flight parameters and UAV-LiDAR and UAV-hyperspectral sensor properties.

Vegetation indices types	Vegetation indices	Formulation	Reference
SR	SR <sub>850,710</sub>	$R_{850}/R_{710}$	[1]
	SR <sub>708,775</sub>	$R_{708}/R_{775}$	[2]
	CI <sub>760,725</sub>	$R_{760}/R_{725} - 1$	[3]
mSR	mSR <sub>800,720</sub>	$(R_{800}-R_{445})/(R_{720}-R_{445})$	[4]
	mCI <sub>800,550</sub>	$(R_{800}-R_{445})/(R_{550}-R_{445}) - 1$	[5]
ND	NDVI	$(R_{830}-R_{660})/(R_{830}+R_{660})$	[6]
	NPCL	$(R_{680}-R_{430})/(R_{680}+R_{430})$	[7]
DD	MTCI	$(R_{754}-R_{709})/(R_{709}-R_{681})$	[8]
	DATT	$(R_{850}-R_{710})/(R_{850}-R_{680})$	[9]

Note: SR = the simple ratio index; mSR = the modified simple ratio index; ND = the normalized difference index; DD = the double difference index.

## References

- Coops, N.C.; Stone, C.; Culvenor, D.S.; Chisholm, L.A.; Merton, R.N. Chlorophyll content in eucalypt vegetation at the leaf and canopy scales as derived from high resolution spectral data. *Tree Physiol.* **2003**, *23*, 23–31, doi:10.1093/treephys/23.1.23.
- Féret, J.-B.; François, C.; Gitelson, A.; Asner, G.P.; Barry, K.M.; Panigada, C.; Richardson, A.D.; Jacquemoud, S. Optimizing spectral indices and chemometric analysis of leaf chemical properties using radiative transfer modeling. *Remote Sens. Environ.* **2011**, *115*, 2742–2750, doi:10.1016/j.rse.2011.06.016.
- Gitelson, A.A.; Keydan, G.P.; Merzlyak, M.N. Three-band model for noninvasive estimation of chlorophyll, carotenoids, and anthocyanin contents in higher plant leaves. *Geophys. Res. Lett.* **2006**, *33*, 2006GL026457, doi:10.1029/2006GL026457.
- Sims, D.A.; Gamon, J.A. Relationships between leaf pigment content and spectral reflectance across a wide range of species, leaf structures and developmental stages. *Remote Sens. Environ.* **2002**, *81*, 337–354, doi:10.1016/S0034-4257(02)00010-X.
- Dong, L.; Long, T.; Zefu, W.; Min, J.; Xia, Y.; Yongchao, T.; Yan, Z.; Weixing, C.; Tao, C. Assessment of unified models for estimating leaf chlorophyll content across directional-hemispherical reflectance and bidirectional reflectance spectra. *Remote Sens. Environ.* **2019**, *231*, doi:10.1016/j.rse.2019.111240.
- Xin, S.; Lin, C.; Coops, N.C.; Hongchao, F.; Xiangqian, W.; Hao, L.; Guibin, W.; Fuliang, C. Quantifying vertical profiles of biochemical traits for forest plantation species using advanced remote sensing approaches. *Remote Sens. Environ.* **2020**, *250*, 112041, doi:10.1016/j.rse.2020.112041.
- Peñuelas, J.; Gamon, J.A.; Fredeen, A.L.; Merino, J.; Field, C.B. Reflectance indices associated with physiological changes in nitrogen- and water-limited sunflower leaves. *Remote Sens. Environ.* **1994**, *48*, 135–146, doi:10.1016/0034-4257(94)90136-8.
- Dash, J.; Curran, P.J. The MERIS terrestrial chlorophyll index. *Int. J. Remote Sens.* **2004**, *25*, 5403–5413, doi:10.1080/0143116042000274015.
- Datt, B. A new reflectance index for remote sensing of chlorophyll content in higher plants: Tests using Eucalyptus leaves. *J. Plant Physiol.* **1999**, *154*, 30–36, doi:10.1016/S0176-1617(99)80314-9.

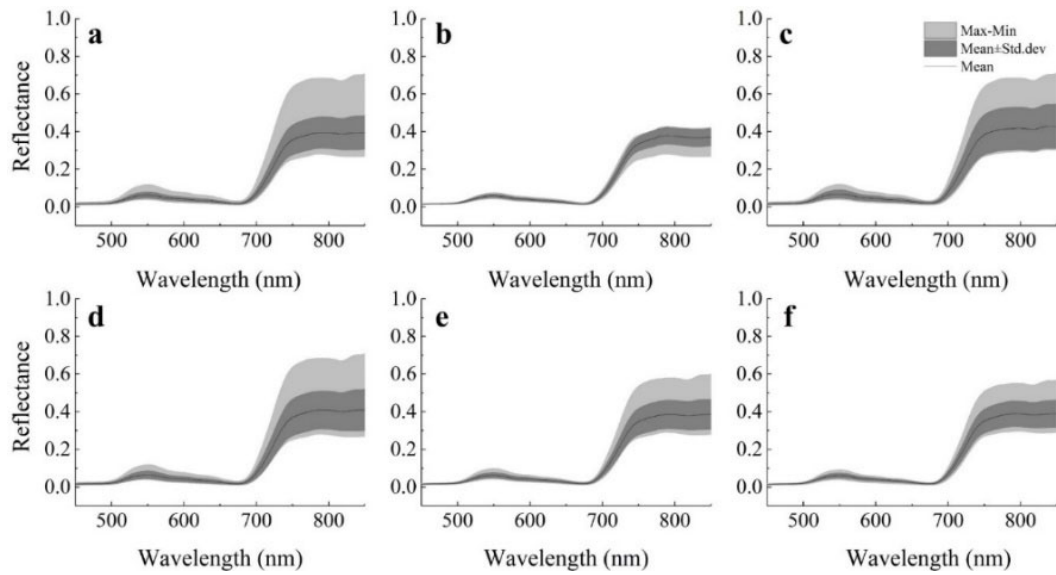


**Figure S1.** Comparison of the maximum-minimum value, mean value and mean  $\pm$  standard deviation of the measured reflectance spectra of the 42 part samples (six parts for seven individual sampling trees). (a): the comparison of the total 42 part samples; (b): the comparison of the 13-year-old part samples; (c): the comparison of the 22-year-old part samples; (d): the comparison of the upper part samples; (e): the comparison of the middle part samples; (f): the comparison of the lower part samples.

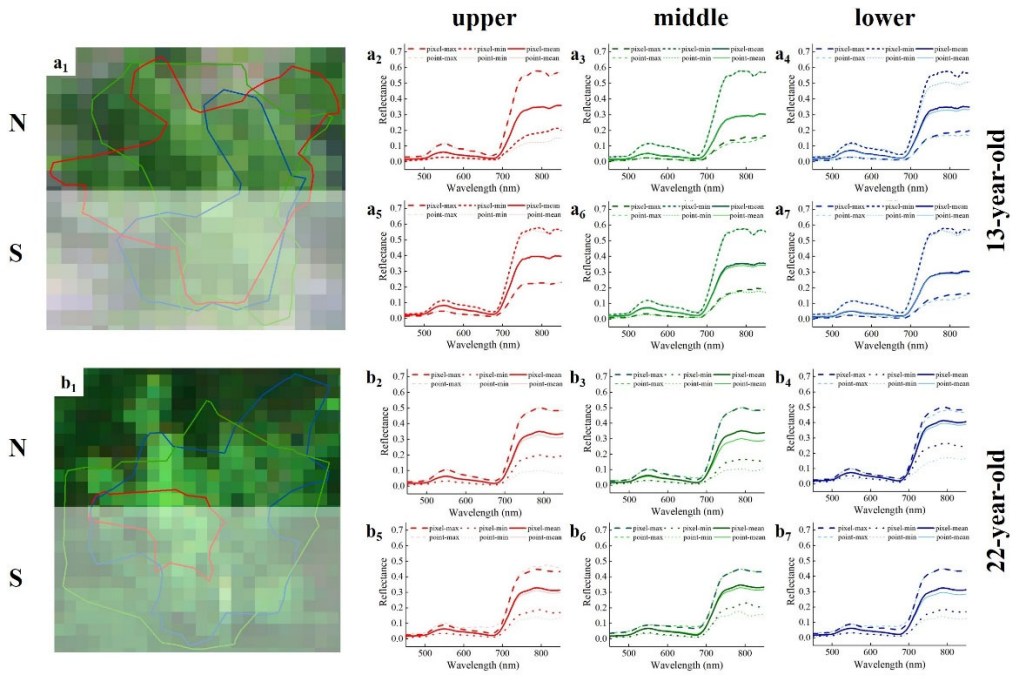


**Figure S2.** The pixel-based and point-based maximum-minimum, mean, and mean  $\pm$  standard deviation reflectance curves for each of the two ages with six part samples. (a<sub>1</sub>, b<sub>1</sub>): the hyperspectral images of sampling tree for 13-year-old and 22-year-old, respectively (the red, green and blue line represent the boundary of the upper, the middle, the lower layer); (a<sub>2</sub>-a<sub>7</sub>): the result of 13-year-old part samples; (b<sub>2</sub>-b<sub>7</sub>): the result of 22-year-old part samples; Note: the “2-7” of alphabetical tab represent the results of the six part samples (i.e., upper north, upper south, middle north, middle south, lower north and lower south); the “pixel-max, pixel-min, pixel-mean” of Figure represent the curve of the max reflectance value, the min reflectance value and the mean reflectance value for the pixel-based, respectively; “point-min, point-min, point-mean” of Figure represent the curve of the max reflectance value, the min reflectance value and the mean reflectance value for the point-based, respectively.

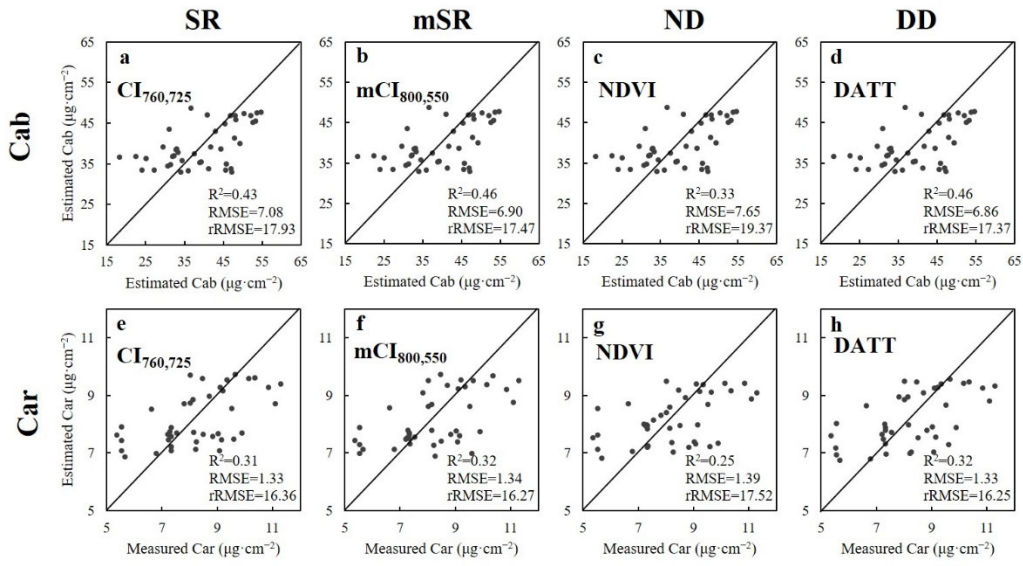


**Figure S3.** Relationship between measured and estimated pigments content based on four types SI models. (a-d): the result of Cab; (e-h): the result of Car; (a, e): the result of SR index; (b, f): the result of mSR index; (c, g): the result of ND index; (d, h): the result of SR index. Note: Cab = total chlorophyll content ( $\mu\text{g}\cdot\text{cm}^{-2}$ ); Car = total carotenoids content ( $\mu\text{g}\cdot\text{cm}^{-2}$ ); SR = the simple ratio index; mSR = the modified simple ratio index; ND = the normalized difference index; DD = the double difference index.